

# Infection of tumor cells with *Salmonella typhimurium* mimics immunogenic cell death and elicits tumor-specific immune responses

Yutaka Horiuchi <sup>a,\*</sup>, Akihiro Nakamura<sup>a</sup>, Takashi Imai <sup>a</sup> and Takashi Murakami <sup>a</sup>

<sup>a</sup>Department of Microbiology, Faculty of Medicine, Saitama Medical University, Saitama 350-0495, Japan

\*To whom correspondence should be addressed: Email: [horchi@saitama-med.ac.jp](mailto:horchi@saitama-med.ac.jp)

Edited By: Karsten Hiller

## Abstract

Some properties of *Salmonella*-infected cells overlap with immunogenic cell death. In this study, we demonstrated that intracellular infection of melanoma with *Salmonella typhimurium* induced high immunogenicity in melanoma cells, leading to antitumor effects with melanoma-antigen-specific T-cell responses. Murine B16F10 melanoma cells were infected with tdTomato-expressing attenuated *S. typhimurium* (VNP20009; VNP-tdT), triggering massive cell vacuolization. VNP-tdT-infected B16F10 cells were phagocytosed efficiently, which induced the activation of antigen-presenting cells with CD86 expression *in vitro*. Subcutaneous coimplantation of uninfected and VNP-tdT-infected B16F10 cells into C57BL/6 mice significantly suppressed tumor growth compared with the implantation of uninfected B16F10 cells alone. Inoculation of mice with VNP-tdT-infected B16F10 cells elicited the proliferation of melanoma-antigen (gp100)-specific T cells, and it protected the mice from the second tumor challenge of uninfected B16F10 cells. These results suggest that *Salmonella*-infected tumor cells acquire effective adjuvanticity, leading to ideal antitumor immune responses.

**Keywords:** antitumor immunity, *Salmonella typhimurium*, intracellular infection, immunogenicity, activation of antigen-presenting cells

## Significance Statement

Antitumor immunity is essential for the therapeutic response to cancer, and its immunogenicity is defined by antigenicity and adjuvanticity. Despite the unique antigenicity of cancer cells, their adjuvanticity remains low. Therefore, to enhance their adjuvanticity, it is necessary to provide appropriate immunogenic cell death (ICD) to cancer cells. The properties of *Salmonella*-infected cells are similar to those of ICDs. After melanoma cells are infected with *Salmonella*, they exhibit ICD-like features, such as increased “find me” signaling, phagocytosis susceptibility, and antigen-presenting cell activation. When these infected cells are inoculated into mice, tumor-antigen-specific T cells proliferate, and strong immune responses can be induced against melanoma. Thus, the immunogenicity of cancer cells using *Salmonella* could be a new module for cancer immunotherapy.

## Introduction

The immune response plays a major role in tumor regression and is crucial for the function of various cancer therapies (1–3). This is evidenced by the fact that conventional anticancer therapy has little effect on tumor regression in immunocompromised hosts (4, 5). Thus, an ideal cancer therapy needs to efficiently damage cancer cells and induce an effective antitumor immune response.

The antitumor immune response can be divided into several steps known as the cancer-immunity cycle (6). The first step in this process is the immunogenic cell death (ICD) of tumor cells (7). Once this occurs, the dead tumor cells are phagocytosed by antigen-presenting cells (APCs) (8, 9). In addition, ICD causes the release of damage-associated molecular patterns (DAMPs), which stimulate APCs (10, 11) and induce the activation of lymphocytes

specific for cancer-derived antigens. These activated lymphocytes then migrate to the tumor sites and attack malignant cells (12). The ICD of tumor cells is characterized by features such as the extracellular secretion of adenosine triphosphate (ATP) (13), activation of inflammasomes (14), secretion of chemokines (e.g. CXCL10 (15)), and expression of “eat me” signals (e.g. calreticulin), which collectively increase the rate of phagocytosis (16). Many of these features are similar to those observed when intracellular parasitic *Salmonella* strains infect mammalian cells (7, 17, 18).

The history of bacterial cancer therapy dates back to the end of the 19th century, when W. B. Coley achieved therapeutic results by administering bacteria to patients with sarcoma (19, 20). Since the beginning of the 21st century, some investigators have re-examined the possibility of treating cancer with bacteria (21). Taking advantage of the tumor-selective property of *Salmonella*,

**Competing Interest:** T.M. has financial interests in Denka Co., Ltd. Y.H., A.N., and T.I. have no financial interest.

**Received:** May 29, 2023. **Accepted:** December 21, 2023

© The Author(s) 2024. Published by Oxford University Press on behalf of National Academy of Sciences. This is an Open Access article distributed under the terms of the Creative Commons Attribution-NonCommercial-NoDerivs licence (<https://creativecommons.org/licenses/by-nc-nd/4.0/>), which permits non-commercial reproduction and distribution of the work, in any medium, provided the original work is not altered or transformed in any way, and that the work is properly cited. For commercial re-use, please contact [journals.permissions@oup.com](mailto:journals.permissions@oup.com)

the antitumor effects of various weakened *Salmonella* strains have been investigated (21). Moreover, modern synthetic biology tools have recently been used to restore the immunosuppressive tumor microenvironment (TME) by programming bacteria to deliver payloads such as short hairpin (sh)RNA and nanobodies to the tumor site and modulate the TME (22–24). However, most of these studies have focused on the tumor cell killing capacity of *Salmonella* strains and not their ability to induce antitumor immunity (25, 26). In addition, almost all of the studies have reported the antitumor effect of the systemic administration of weakened *Salmonella* strains to mice (27, 28), whereas the immunogenicity of tumor cells infected with *Salmonella* has not been assessed in detail.

Effective cancer therapy requires the induction of ICD in tumor cells. However, it is difficult to induce tumor cell ICD in refractory malignancies, such as melanoma, because they are highly resistant to irradiation and many chemotherapeutic agents (29–31). In this study, we demonstrated that the characteristics of intracellular infection of murine B16F10 melanoma cells with attenuated *Salmonella typhimurium* in vitro were consistent with those of ICD. Moreover, the increased immunogenicity of the *S. typhimurium*-infected tumor cells was based on these ICD characteristics.

## Results

### Efficacy of VNP-tdT-mediated B16F10 melanoma cell infection

To investigate the efficacy of melanoma cell infection with attenuated *S. typhimurium*, we first established the VNP-tdT strain, in which the tdTomato (tdT) gene (encoding a red fluorescent protein, RFP) was transfected into the VNP20009 *S. typhimurium* strain. The percentage of RFP<sup>+</sup> and thus *S. typhimurium*-infected cells was measured by flow cytometry. The VNP-tdT strain was then inoculated into a culture system of B16F10 cells at a multiplicity of infection (MOI) 10, 100, and 1,000; an MOI of 1,000 for 5 h led to 100% transfection (Fig. 1A). Confocal laser microscopy confirmed the intracellular localization of VNP-tdT in B16F10 cells (Fig. 1B and Movie S1). We also generated a control *Salmonella* strain, VNP-ctrl, lacking tdTomato from the vector plasmid, and compared its efficiency of infection of B16F10 cells with the VNP-tdT strain. The infection efficiency of VNP-ctrl was equivalent to that of VNP-tdT (Fig. S1).

Previous reports have shown that intracellular infection with *Salmonella* activates the inflammasome of mammalian cells (32, 33). Therefore, to confirm the response to intracellular VNP-tdT infection, caspase-1 activity was measured in VNP-tdT-infected B16F10 cells. Indeed, we found that caspase-1 activity was higher immediately after VNP-tdT infection and further increased as infection progressed (Fig. 1C and D). To verify that this response was not specific to B16F10 cells, the activation of caspase-1 by VNP-tdT infection was also observed in five human malignant melanoma cell lines (Fig. S2). Moreover, the inoculation of B16F10 cells with *Escherichia coli* or heat-killed VNP-tdT did not lead to caspase-1 activation (Fig. 1C and D).

### *Salmonella*-mediated tumor cell degeneration

Intracellular vacuoles were detected in VNP-tdT-infected cells at about 3 h postinfection. Moreover, many of the infected cells showed signs of degeneration, with large vacuoles appearing at 5 h postinfection (Fig. 1E and F and Movie S1 [shown by the arrow]). This vacuolar-associated degeneration of tumor cells was not observed following infection with *E. coli* or heat-killed VNP-tdT (Fig. 1F), suggesting that vacuole formation was

associated with intracellular *S. typhimurium* invasion. The efficiency of vacuolar degeneration associated with VNP-ctrl was equivalent to that of VNP-tdT (Fig. S3).

Methuosis is a type of cell death characterized by excessive vacuolization of the cytoplasm (34, 35), which results from increased macropinocytosis. To further confirm whether the large vacuoles found in the VNP-tdT-infected tumor cells were due to macropinocytosis, B16F10 cells were infected with VNP-tdT in the presence of Lucifer Yellow, a fluid-phase tracer that is internalized via an endocytic process. Fluorescence microscopy showed that the intracellular vacuoles were filled with extracellular fluid containing Lucifer Yellow (Fig. 2A). These results indicate that the large vacuoles formed in the VNP-tdT-infected B16F10 cells were macropinosomes. The activation of Rac1 is essential for micropinocytosis (36). Moreover, Bhanot et al. (37) reported that a specific inhibitor of Rac1, EHT1864, suppresses methuosis. Therefore, we examined the effect of EHT1864-mediated Rac1 inhibition on infected tumor cells. We found no noticeable difference between tumor cells treated with EHT1864 and those treated with the solvent control (Fig. S4). However, when B16F10 cells were infected with VNP-tdT in the presence of EHT1864, most of the infected cells died at a time point when vacuolization would normally be evident in the absence of EHT1864 (Fig. 2B and C); only a few live cells remained at 5 h postinoculation. Thus, unlike methuosis, the accompanying increase in macropinocytosis observed in infected tumor cells may play a role in resisting cell death.

Next, we performed a microarray analysis of the transcriptome. As shown in Fig. 2D, an increase in *Cyr61* mRNA expression was observed at 3 h postinfection. *Cyr61* is associated with Rac1 activation (38) and affects features of the immune response such as leukocyte trafficking (39) and interferon responses (40, 41). The UCSC Xena (<https://xena.ucsc.edu>) platform was subsequently used to analyze data from The Cancer Genome Atlas-registered human melanoma dataset. We found a significant positive correlation between the expression of *Cyr61* and that of the lymphocyte activation marker CD69 ( $r = 0.3575$ ,  $P = 1.820 \times 10^{-15}$ , Pearson's rho; Fig. S5). Thus, focusing on the expression of genes related to ICD and innate immunity, we confirmed that the expression of these genes fluctuated with *S. typhimurium* infection and served to enhance the immune response (Fig. 2E).

These results suggest that infected melanoma cells that exhibited vacuolar degeneration resisted cell death as well as having phenotypes that elicited a host immune response. Recent studies have shown that residual tumor cells injured by exposure to a stressor are more immunogenic than dead cells (42, 43). Thus, all of the above factors raised the possibility that the infection of tumor cells with *Salmonella* was the initiating step of the antitumor response.

### Efficient phagocytosis of infected tumor cells by APCs induces their activation

Next, we examined whether VNP-tdT-infected tumor cells were recognized by immune cells. Degenerating cells release “find me” signals, such as extracellular ATP (44), which attract phagocytes. Moreover, extracellular ATP concentrations are elevated in various types of cellular injury (45). Indeed, we found that ATP concentration in B16F10 cell culture supernatants was higher upon infection with VNP-tdT (Fig. 3A).

Once phagocytes reach their target cells by responding to “find me” signals, phagocytosis cannot be initiated if the target cells express “don't eat me” signals. The typical “don't eat me” signal

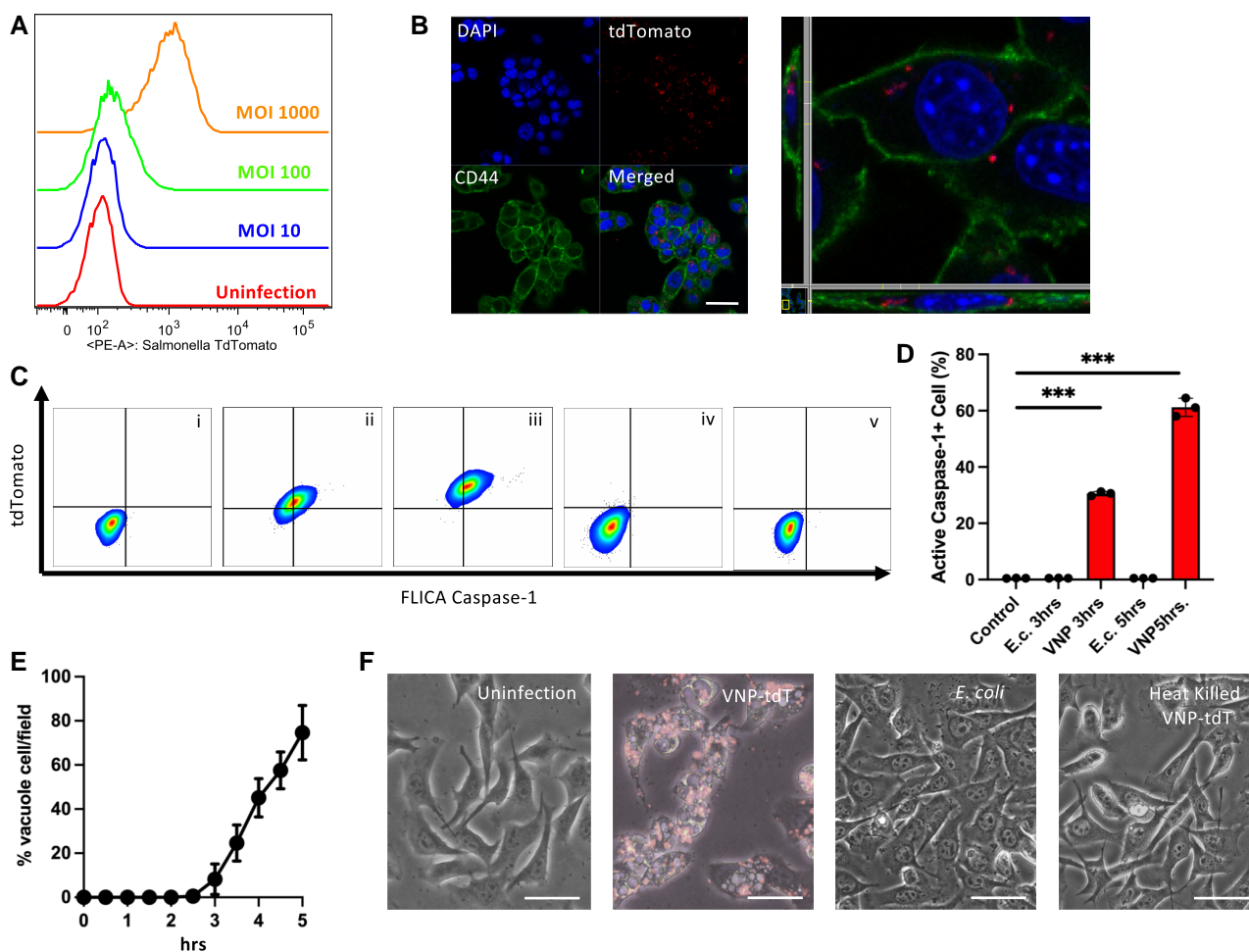


**Fig. 1.** Intracellular VNP-tdT infection causes tumor cell vacuolization. B16F10 cells were infected with VNP-tdT at an MOI 10, 100, or 1,000. A) A flow cytometry histogram showing the infection efficiency at various MOIs. B) A confocal laser microscopy image showing intracellular infection of B16F10 cells with VNP-tdT; DAPI was used to stain the nuclei, CD44 to stain the plasma membrane, and tdTomato to localize *Salmonella*. Scale bar = 50  $\mu$ m. C) Representative flow cytometry density plots of caspase-1 activity (FLICA) vs. the tdTomato signal (bacteria) in B16F10 under the following experimental conditions: (i) uninfected; (ii) VNP-tdT-infected for 3 h; (iii) VNP-tdT-infected for 5 h; (iv) cocultured with tdTomato-expressing *E. coli* for 5 h; and (v) cocultured with heat-killed VNP-tdT for 5 h. D) A quantification of the percentage of cells that exhibited caspase-1 activity. Data are shown as the mean  $\pm$  SD in the panels ( $n = 3$  per group). Statistical significance was determined using one-way ANOVA, in comparison with the control ( $***P < 0.001$ , Dunnett's test). E) Changes with time in the percentage of vacuolized VNP-tdT-infected B16F10 cells. Vacuolized cells were counted using a microscope. Data are shown as the mean  $\pm$  SD in the panels (10 fields per group). F) A representative image of vacuolization. Scale bar = 50  $\mu$ m.

molecule CD47 binds to signal-regulatory protein  $\alpha$  (SIRP $\alpha$ ), which is highly expressed on the cell surface of macrophages and dendritic cells (DCs) and negatively regulates phagocytosis (46). CD47 is highly expressed in a variety of cancers, including melanoma, and promotes immunological escape by preventing APC-mediated phagocytosis via SIRP $\alpha$ . Because the microarray analysis results showed that *Salmonella* infection reduced the expression of CD47 (Fig. 2E), we evaluated CD47 expression by flow cytometry. CD47 expression was lower in VNP-tdT-infected than in uninfected B16F10 cells (Fig. 3B). These results support the notion that CD47 expression on the surface of B16F10 cells was negatively regulated by infection with VNP-tdT.

Gardai et al. (47) reported that decreased CD47 expression, coupled with "eat me" signaling by calreticulin expressed in target cells, promotes phagocytosis. Therefore, we next examined whether B16F10 cells infected with VNP-tdT exposed calreticulin to the cell surface. There was no difference between infected and uninfected cells, and we could not confirm whether *Salmonella* infection enhanced calreticulin expression on the surface of melanoma cells (Fig. S6). Feng et al. (48, 49) reported that

calreticulin exposure on the surface of macrophages acts as a guide for recognizing tumor cells and promoting phagocytosis. Thus, we cocultured VNP-tdT-infected B16F10 cells with the mouse macrophage cell line Raw264.7 and examined the exposure of calreticulin to the surface of Raw264.7 cells. Compared with Raw264.7 cells cocultured with uninfected B16F10, Raw264.7 cells cocultured with VNP-tdT-infected B16F10 had higher calreticulin surface levels (Fig. 3C), meaning that they were more likely to recognize and phagocytose tumor cells. These results suggest that *Salmonella* infection of tumor cells promoted their recognition by the host immune system.

We next examined changes in the sensitivity of B16F10 cells to phagocytosis induced by VNP-tdT infection. It was previously reported that MC38 mouse colon cancer cells infected with *Salmonella* release ATP and are phagocytosed by bone-marrow-derived macrophages (50). However, the above study only monitored changes in interleukin (IL)-1 $\beta$  production in the presence or absence of cytochalasin D; therefore, the results are only indirect evidence of the phagocytosis of infected tumor cells. Thus, to investigate the phagocytosis of infected tumor cells directly, we

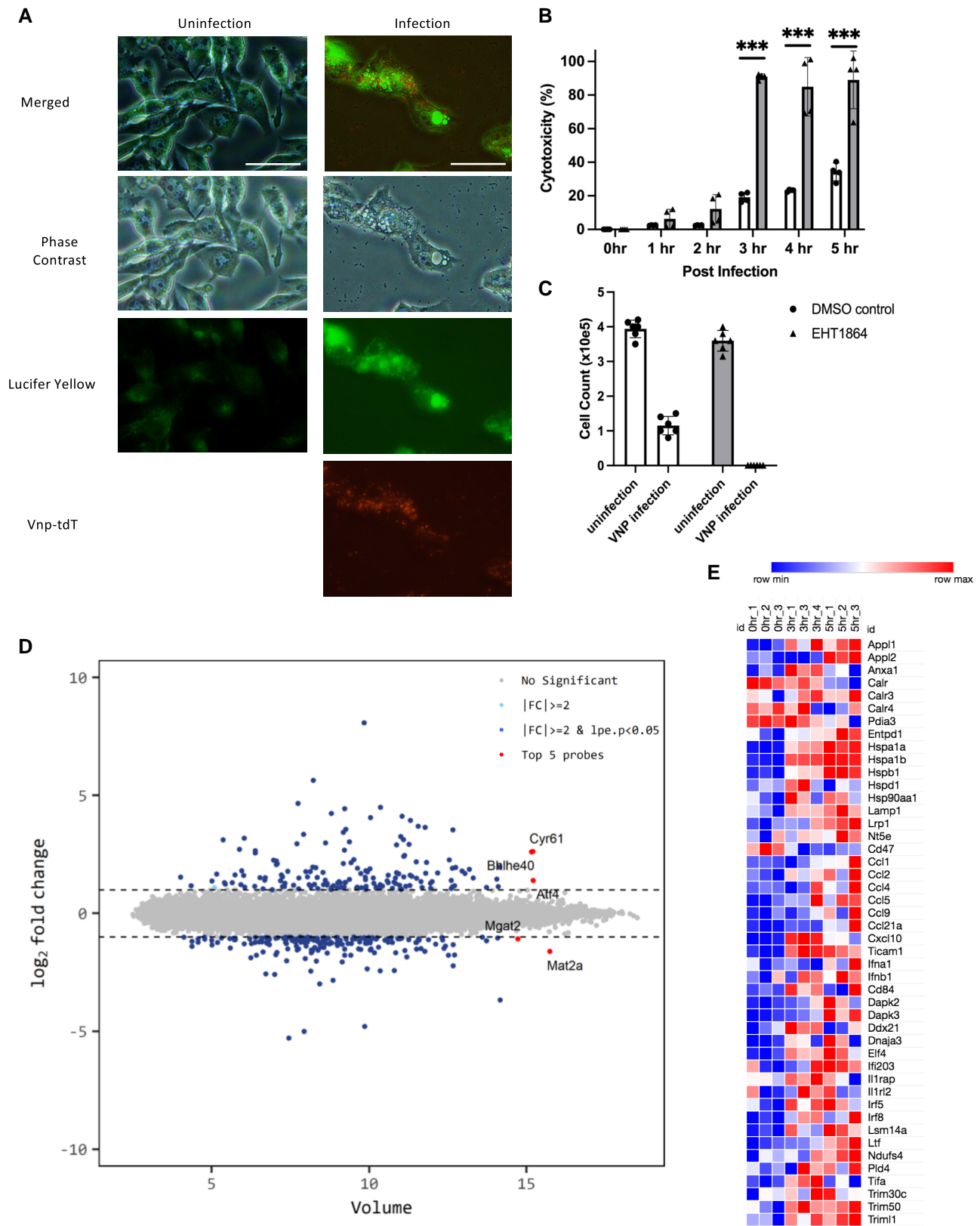


**Fig. 2.** Cellular degeneration and gene expression induced by VNP-tdT infection. B16F10 cells were infected with VNP-tdT at an MOI of 1,000. A) The vacuoles of VNP-tdT-infected B16F10 cells incorporated the extracellular fluid-phase tracer Lucifer Yellow. Scale bar = 50  $\mu$ m. Trends in cell death with time B) and the number of live cells at 5 h postinfection C) after blocking Rac1 activation. Data are shown as the mean  $\pm$  SD in the panels ( $n = 3$  per group). Statistical significance was determined using the Student's  $t$  test; the EHT1864 group was compared with the DMSO control group ( $***P < 0.001$ ). D) A transcriptome analysis using a DNA microarray; gene expression at 3 h postinfection was compared against the control. E) The expression levels (measured using the DNA microarray) of ICD- and innate-immunity-related genes in the control vs. 3 and 5 h postinfection.

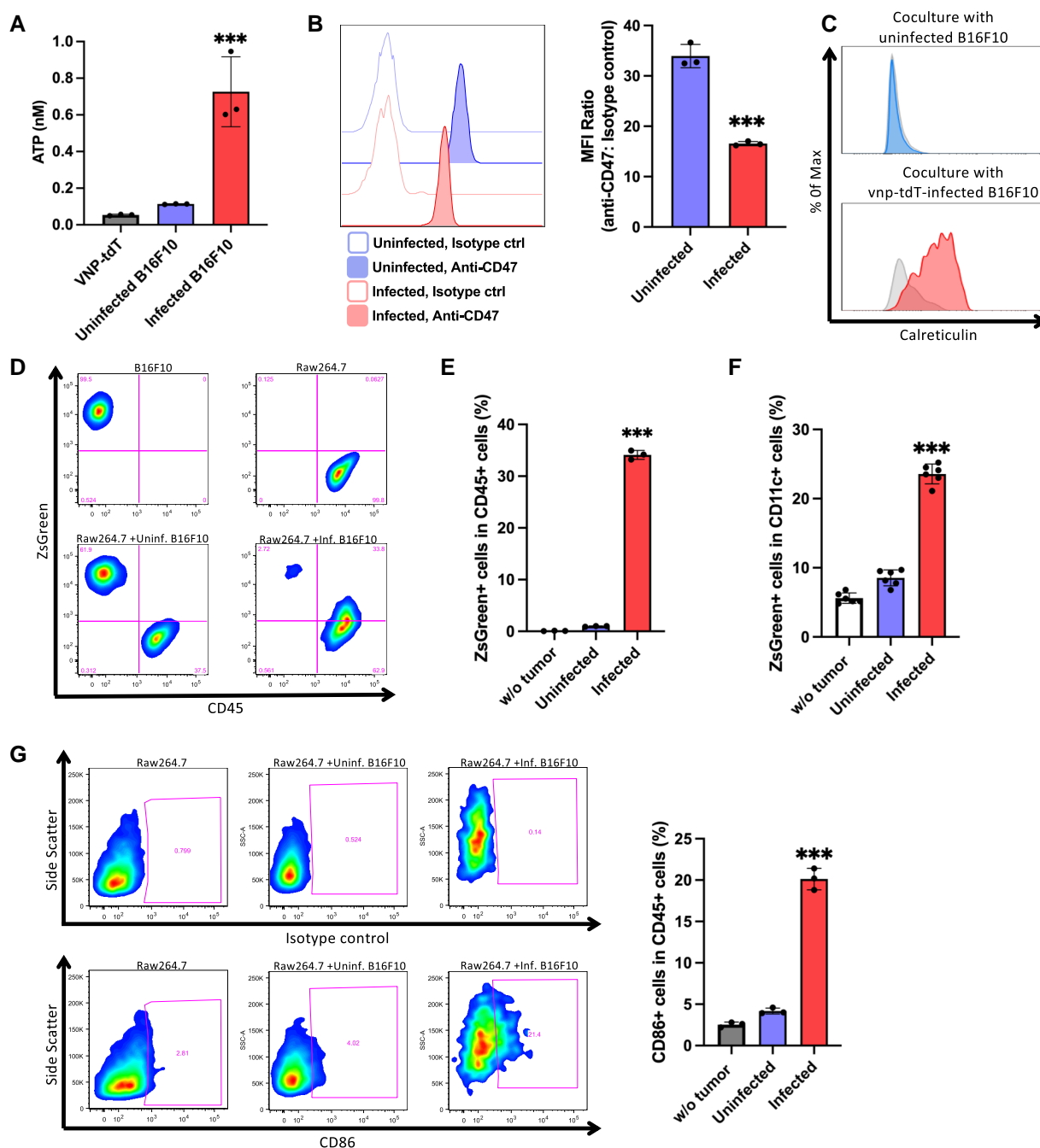


**Fig. 3.** *Salmonella*-infected melanoma cells have the characteristics of cells undergoing ICD. A) The levels of extracellular ATP in the conditioned medium. Statistical significance was determined using one-way ANOVA; VNP-tdT-infected and uninfected B16F10 cells were compared ( $***P < 0.001$ , Dunnett's test). B) The cell surface CD47 expression of uninfected and infected B16F10 cells. A representative histogram (left panel) and comparison of mean fluorescent intensity between uninfected and infected B16F10 cells. Data are shown as the mean  $\pm$  SD in the panels ( $n = 3$  per group). Statistical significance was determined using the Student's  $t$  test; VNP-tdT-infected and uninfected B16F10 cells were compared ( $***P < 0.001$ ). C) The cell surface calreticulin exposure levels of Raw264.7 macrophages cocultured with uninfected (upper panel) or VNP-tdT-infected (lower panel) B16F10 cells. The gray histogram indicates isotype-control staining. D–F) A flow cytometric analysis of phagocytosis by Raw264.7 macrophages (D, E) and BMDCs (F). Phagocytes were cocultured with uninfected or VNP-tdT-infected B16F10 cells expressing ZsGreen. Representative flow cytometry plots and data quantification are shown. Data are shown as the mean  $\pm$  SD in the panels ( $n = 3$  [Raw264.7] or  $n = 4$  [BMDC] per group). Statistical significance was determined using one-way ANOVA; VNP-tdT-infected and uninfected B16F10 cells were compared ( $***P < 0.001$ , Dunnett's test). G) A flow cytometric analysis of CD86 (an APC activation marker) expression by Raw264.7 macrophages cocultured with uninfected or VNP-tdT-infected B16F10 cells. Representative flow cytometry plots and data quantification are shown. Data are shown as the mean  $\pm$  SD in the panels ( $n = 3$  per group). Statistical significance was determined using one-way ANOVA; VNP-tdT-infected and uninfected B16F10 cells were compared ( $***P < 0.001$ , Dunnett's test).

cocultured VNP-tdT-infected ZsGreen-expressing B16F10 cells with Raw264.7 cells or mouse bone-marrow-derived DCs (BMDCs) and assessed the percentage of phagocytes that incorporated tumor-cell-derived ZsGreen (Fig. 3D). VNP-tdT-infected cells

were phagocytosed by Raw264.7 cells more efficiently than uninfected cells (Fig. 3E). Similar results were observed in the coculture experiments with mouse BMDCs (Fig. 3F). Furthermore, an increase in the expression of the costimulatory molecule CD86

was also observed in Raw264.7 cells cocultured with infected B16F10 cells (Fig. 3G). These findings suggest that intracellular infection with *Salmonella* enhanced the engraftment sensitivity of tumor cells and subsequently increased their adjuvanticity and immunogenicity.

### Tumor growth suppression by VNP-tdT-infected B16F10 cells

To investigate whether infection of tumor cells with *Salmonella* affected their growth in vivo, we subcutaneously injected a mixture of VNP-tdT-infected and uninfected B16F10 cells into mice. Tumor formation was markedly suppressed in the group inoculated with infected B16F10 cells alone (Fig. 4A). Compared with the group inoculated with uninfected cells alone, the group inoculated with a mixture of VNP-tdT-infected cells (at a 4:1 or 1:1 ratio of uninfected to infected B16F10 cells) had significantly reduced tumor growth (Fig. 4B) and prolonged survival (Fig. 4C). Notably, no significant differences in tumor growth were observed between mice inoculated with B16F10 cells infected with VNP-ctrl and those inoculated with B16F10 cells infected with VNP-tdT (Fig. S7). These results suggest that the presence of VNP-tdT-infected B16F10 cells inhibited tumor growth. Because the host antitumor immune response is involved in the suppression of tumor growth, it is possible that mice inoculated with VNP-tdT-infected B16F10 cells had established an immune memory against the B16F10 melanoma cell line. Thus, we next evaluated the immune memory status of mice by rechallenging mice that had not developed tumors after 14 days of subcutaneous inoculation with uninfected and VNP-tdT-infected B16F10 cells (mixed at ratios of 4:1 or 1:1) with uninfected B16F10 cells alone (Fig. 4D). Compared with naïve mice, the mice that did not form tumors after the initial inoculation had suppressed tumor growth 15 days after rechallenge (Fig. 4E). Suppression of tumor growth after rechallenge suggests that inoculation with VNP-tdT-infected B16F10 cells induced a melanoma-antigen-specific immune response.

### Inoculation of model mice with VNP-tdT-infected B16F10 cells induces an effective antimelanoma cytotoxic T-cell response

We next examined how infection of B16F10 cells with *Salmonella* affected the cytotoxic T lymphocyte (CTL)-mediated tumor-specific immune responses. We performed a CTL assay using lymphocytes derived from mice inoculated with VNP-tdT-infected or mitomycin-C-treated B16F10 cells. Compared with lymphocytes from the mitomycin-C-treated B16F10-inoculated mice, lymphocytes from the VNP-tdT-infected B16F10-inoculated mice exhibited increased cytotoxic activity against B16F10 cells (Fig. 5A and B). The cytotoxic activity of these lymphocytes was significantly lower when Ex3LL lung carcinoma or RMA lymphoma cells, rather than B16F10 cells, were used as targets (Fig. 5B). These results indicate that the inoculation of VNP-tdT-infected B16F10 cells induced an immune response specific to melanoma-cell-derived antigens.

We further validated our observations using Pmel-1 mice, which harbor lymphocytes recognizing the melanoma-associated antigen, gp100 (51, 52). The antigen-specific activation and proliferation of lymphocytes in vivo was monitored using Ki67 expression (53). We observed an increase in Ki67 levels in lymphocytes derived from Pmel-1 mice inoculated with VNP-tdT-infected B16F10 cells than those obtained from mice immunized with mitomycin-C-treated B16F10 cells (Fig. 5C and D; see Materials

and methods section). Previous studies reported that the expression of fluorescent proteins in tumor cells might increase tumor immunogenicity, leading to the control of tumor growth and modulation of the TME (54, 55). Therefore, we investigated whether the elicitation of melanoma-antigen-specific immune responses depended on the presence or absence of fluorescent proteins derived from bacteria that infected the tumor cells. As shown in Fig. S8, there were no significant differences in the expression level of Ki67 in gp100-specific CD44<sup>+</sup>CD8<sup>+</sup> lymphocytes in Pmel-1 mice inoculated with B16F10 cells infected with VNP-ctrl compared with those inoculated with B16F10 cells infected with VNP-tdT. These results suggest that the expression of fluorescent proteins by bacteria that infected tumor cells had little impact on modifying tumor immunogenicity. Thus, these results demonstrate that VNP-infected B16F10 cells elicited a strong melanoma-antigen-specific immune response and hampered melanoma progression.

## Discussion

In this report, we aimed to elicit a superior antitumor immune response by infecting tumor cells with *Salmonella*. We determined the in vitro infection conditions under which the attenuated *S. typhimurium* strain VNP-tdT infected almost all B16F10 cells. Under these conditions, infected B16F10 cells exhibited cell degeneration, with extensive vacuole formation. We showed that the vacuoles were macropinosomes, and that the inhibition of Rac1, which induces macropinosomes, caused the rapid death of VNP-tdT-infected cells. This suggested that the vacuolization seen in VNP-tdT-infected cells was not a phenotype of programmed cell death (e.g. methuosis), but instead rendered tumor cells more resistant to cell death and slowed cell death progression. Sriram et al. (43) reported that injured living cells are more immunogenic than dead cells. Thus, slowing down cell death progression should improve the immune response against cancer cells. Moreover, we observed that *Salmonella*-infected tumor cells exhibited characteristics reminiscent of ICD, such as the higher secretion of “find me” signals, susceptibility to phagocytosis, and APC activation (Fig. 3). This indicated that *Salmonella*-infected tumor cells effectively stimulated antitumor immunity. Moreover, the inoculation of mice with these infected cells induced immunity against malignant melanoma tumors (Fig. 5).

The immunogenicity of cells is defined by both antigenicity and adjuvanticity (56). In general, cancer cells have unique antigenicity, as they express novel antigens, such as tumor neoantigens (TNAs), which are derived from somatic mutations, and tumor-associated antigens (TAAs), which are differentiation antigens specific to the cell lineage of origin (e.g. gp100). However, the adjuvanticity of malignant cells is very low and close to that of normal cells. Therefore, tumor cells are not easily phagocytosed, while APCs that have phagocytosed tumor cells are not sufficiently activated. As a result, immunological ignorance and peripheral immune tolerance are established (57–59). Thus, the aim of developing therapies to induce ICD is to enhance the low adjuvanticity of cancer cells (7, 57). DAMPs (e.g. ATP and high mobility group box [HMGB]-1) released by cells undergoing ICD promote the recruitment of phagocytically competent APCs and elicit sufficient antigen-presenting capacity to activate antigen-specific lymphocytes. APCs express pattern recognition receptors such as Toll-like receptors, which bind not only to DAMPs but also to various pattern-associated molecular patterns (PAMPs). PAMPs are derived from microbial components and induce a series of responses ranging from APC activation to enhancing antigen

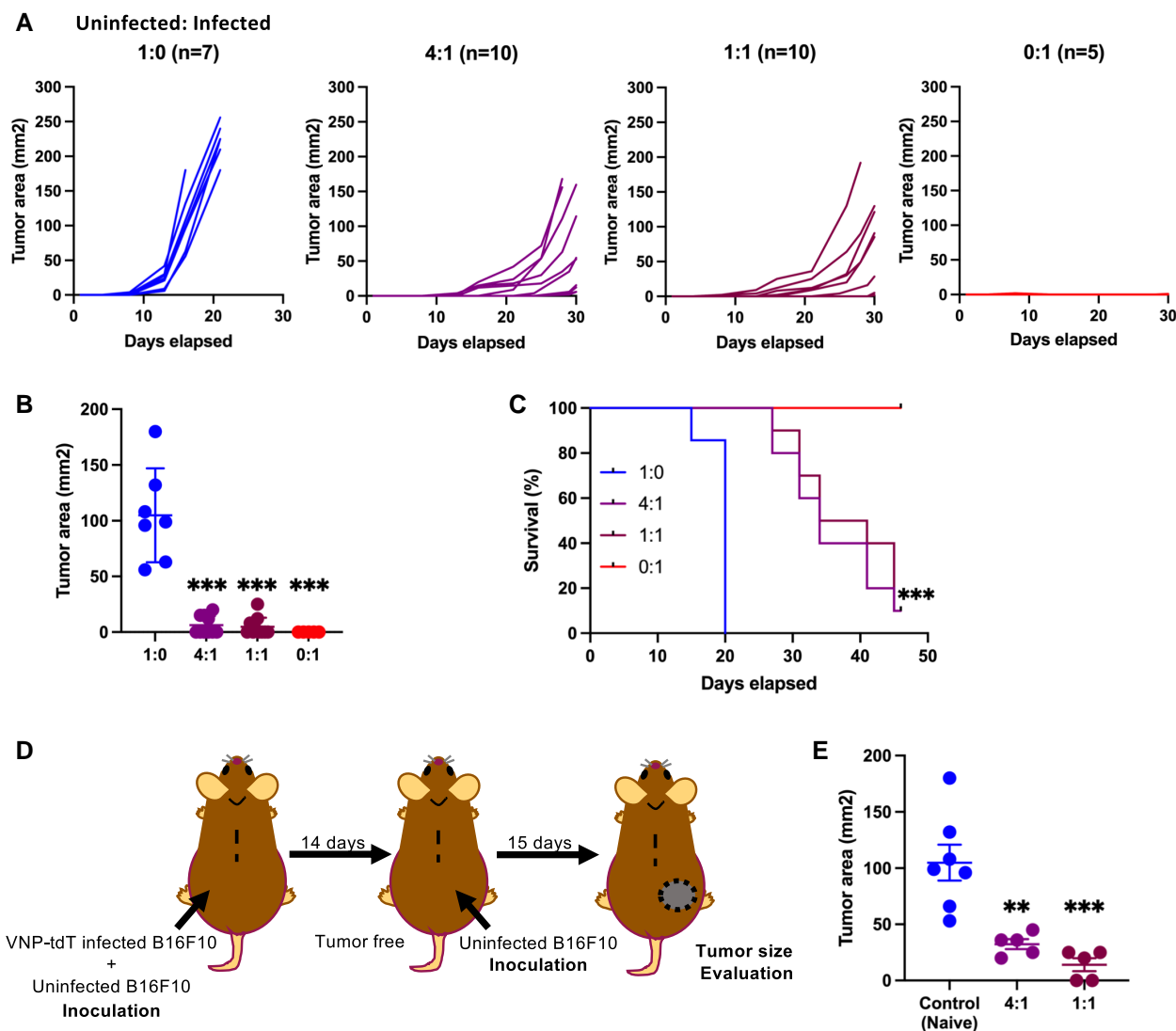


**Fig. 4.** The presence of *Salmonella*-infected melanoma cells inhibits melanoma progression. A–C) Mice were inoculated with a mixture of VNP-tdT-infected and uninfected B16F10 cells. Tumor volume (A and B) and mouse survival (C) were monitored. In (B), the data are presented as the mean  $\pm$  SD. Statistical significance was determined using one-way ANOVA; naïve mice were the comparator group (\*\* $P < 0.001$ , Dunnett's test). In (C), the data are analyzed using the log-rank test (\*\* $P < 0.001$ ). D) An outline of the cancer immunization protocol used in this study. E) Individual secondary tumor sizes from naïve mice or mice immunized with a mixture of VNP-tdT-infected and uninfected B16F10 cells; data are presented as the mean  $\pm$  SD. Statistical significance was determined using one-way ANOVA; naïve mice were the comparator group (\*\* $P < 0.01$ , \*\*\* $P < 0.001$ , Dunnett's test).

presentation. Indeed, in our study, *Salmonella*-infected tumor cells were phagocytosed at a higher rate than uninfected tumor cells, leading to the activation of cocultured APCs (Fig. 3D–G) and the proliferation of lymphocytes recognizing the melanoma antigen, gp100, in vivo (Fig. 5C). This is evidence for the induction of an ICD-like immune response by the bacterial infection of tumor cells.

Microbial infection triggers lymphocyte responses to host-cell-derived antigens. Moreover, the nonspecific activation of the innate immune system by infectious agents leads to the breakdown of peripheral immune tolerance and the activation of autoreactive T cells that escape central immune tolerance (60). For instance, myelin-specific T-cell receptor transgenic mice, a model of multiple sclerosis (an autoimmune neurological disease), do not develop experimental autoimmune encephalomyelitis (EAE) in a specific-pathogen-free environment, but spontaneously develop EAE in a conventional environment (61). A similar mechanism has been observed in antitumor immune responses. For instance, Overwijk

et al. (62) demonstrated that in Pmel-1 mice, which harbor T cells specific for gp100 (a tissue differentiation antigen associated with melanocytes), these gp100-specific T cells normally exist in an inactive state and are not activated by the level of gp100 antigen presented in vivo. However, when the Pmel-1 mice are exposed to total body irradiation, bacterial translocation from the damaged intestinal tract activates gp100-specific T cells and triggers an antimelanoma immune response (63). These results indicate that peripheral immune tolerance, which suppresses the activation of antigen-specific T cells present in the body, breaks down upon infection (64). In our study, we confirmed that the inoculation of *Salmonella*-infected B16F10 cells into Pmel-1 mice induced the proliferation of gp100-specific T cells in vivo. Taken together, these findings indicate that bacterial infection triggers strong immune responses against TAAs, as well as the activation of autoreactive T cells.

TNAs, generated by the genetic mutation of tumors, are not expressed in normal cells and are therefore not subject to central immune tolerance; the same applies to antigens of microbial

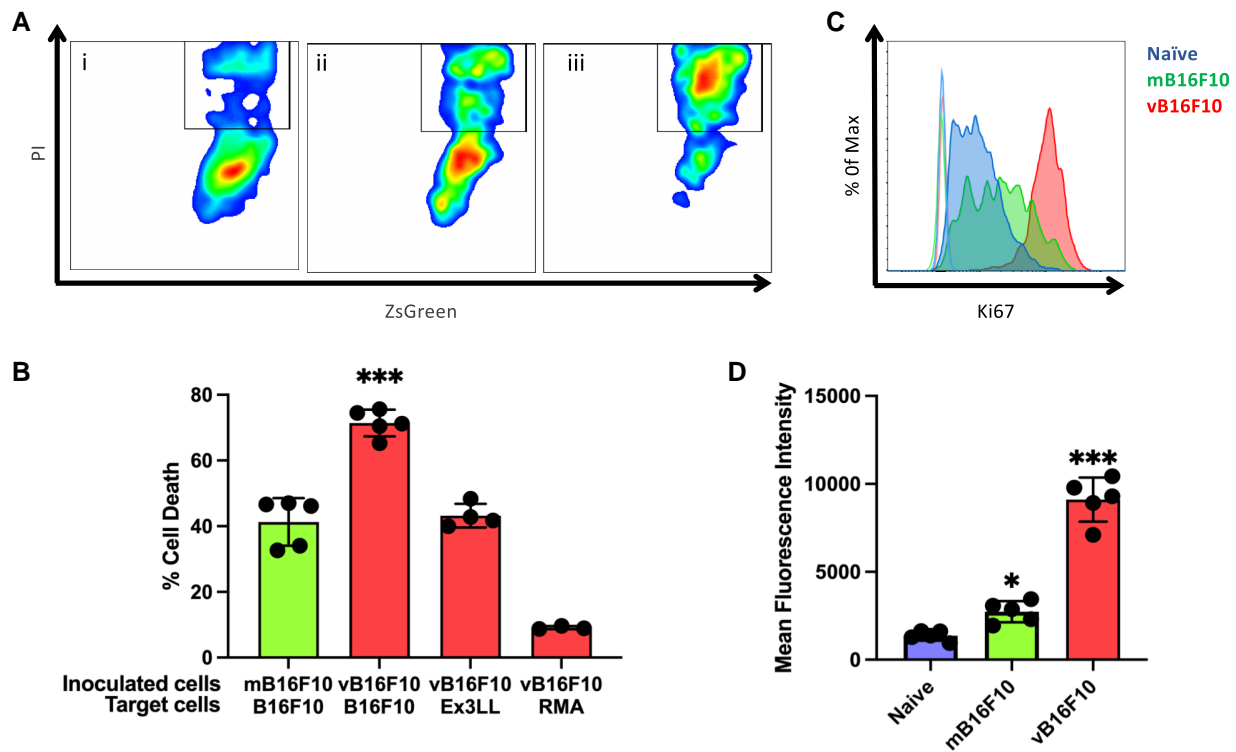


**Fig. 5.** Immunization with *Salmonella*-infected melanoma cells promotes antimelanoma immune responses. A and B) A flow cytometric analysis of the cytotoxicity of lymphocytes, derived from mice inoculated with VNP-tdT-infected (vB16F10) or mitomycin C-treated (mB16F10) B16F10 cells, against B16F10. Representative flow cytometry plots and data quantification are depicted. Data are shown as the mean  $\pm$  SD in the panels ( $n = 5$  [mB16F10-B16F10],  $n = 5$  [vB16F10-B16F10],  $n = 4$  [vB16F10-Ex3LL],  $n = 3$  [vB16F10-RMA] per group). Statistical significance was determined using one-way ANOVA; lymphocytes derived from the mB16F10-challenged mice were used as the comparator group ( $***P < 0.001$ , Dunnett's test). C and D) An evaluation of melanoma-antigen-specific CD8<sup>+</sup> T-cell proliferation. Representative flow cytometry plots showing the Ki67 expression of gp100-MHC-tetramer<sup>+</sup> CD44<sup>+</sup> CD8<sup>+</sup> lymphocytes derived from Pmel-1 mice inoculated with vB16F10 or mB16F10; data are presented as the mean fluorescence intensity of Ki67 staining. Data are shown as the mean  $\pm$  SD in the panels ( $n = 5$ ). Statistical significance was determined using one-way ANOVA; lymphocytes derived from naïve Pmel-1 mice were used as the comparator group ( $*P < 0.05$ ,  $***P < 0.001$ , Dunnett's test).

origin. In this case, T cells with TNA-specific T-cell receptors are not eliminated by the thymus and remain in the periphery (64). Therefore, we can speculate that if improving the adjuvanticity of tumor cells by intracellular *Salmonella* infection elicits an immune response to TAAs that are also expressed on normal cells, such as gp100, then an immune response can be elicited not only against TAA but also against TNA expressed on the same cells as TAA. Thus, the infection of tumor cells with *Salmonella* and other microorganisms may trigger the induction of an immune response with a broad antigenic spectrum that includes low-antigenic epitopes such as TAAs and high-antigenic epitopes such as TNAs. An antitumor immune response with a broad antigen spectrum is expected to reduce the chance of tumor immune escape and result in more effective tumor elimination. In relation to the present study, it remains to be examined whether the inoculation of *Salmonella*-infected melanoma cells into mice would induce an immune response against TNAs and TAAs other than gp100. It would also be interesting to determine the range of the epitope spectrum of the induced immune response. However, our results indicate that the inoculation of VNP-tdT-infected cells induced potent CTL activity against B16F10 cells, and specifically against gp100, a TAA (Fig. 5C). Thus, it is reasonable to assume that an immune response against TNAs derived from B16F10 cells was also elicited and contributed to the potency of CTL-mediated melanoma cell eradication.

In conclusion, intracellular infection with *Salmonella* enhanced the immunogenicity of melanoma cells. The application of *Salmonella* as a modern biology tool for manipulating tumor cells

and inducing potent antitumor immunity may therefore represent an effective cancer treatment strategy.

## Materials and methods

### Animals and cell lines

C57BL/6J mice were purchased from Charles River Laboratories Japan, Inc. (Yokohama, Japan). B6.Cg-Thy1a/Cy Tg(TcraTcrb)8Rest/J mice (51, 52) were originally purchased from The Jackson Laboratory (JAX stock #005023; Bar Harbor, ME, USA). Eight- to 12-week-old mice were used for all experiments. Mice were housed in an appropriate animal care facility at Saitama Medical University (Saitama, Japan) and handled according to international guidelines for experiments on animals. The Animal Care and Use Committee of Saitama Medical University (Saitama, Japan) approved the procedures for this study (approval nos. 3740 and 3742).

The B16F10 mouse melanoma, MM-RU human melanoma, and Raw264.7 mouse macrophage cell lines were cultured in vitro in Dulbecco's modified Eagle medium (DMEM; Nacalai Tesque, Kyoto, Japan) supplemented with 10% fetal bovine serum (FBS). The C32TG, G361, SK-MEL-2, and SK-MEL-28 human melanoma cell lines were cultured in vitro in Eagle's minimum essential medium (Nacalai Tesque) supplemented with 10% FBS. To generate B16F10 cells expressing the green fluorescent protein ZsGreen, the lentiviral vector pLVSIIN-ZsGreen (Clontech, Mountain View, CA, USA) was used in accordance with the manufacturer's instructions.

## Bacteria

To generate tdTomato-expressing *S. typhimurium* (VNP-tdT), the ptdTomato vector (Clontech) was electroporated into the *S. typhimurium* strain VNP20009 (obtained from American Type Culture Collection, Manassas, VA, USA) using a Genepulser Xcel electroporator (Bio-Rad, Hercules, CA, USA) at 2.5 kV, 1,000  $\Omega$ . VNP-ctrl, a control transfectant *S. typhimurium*, was generated by transfection of the vector plasmid without tdTomato. Transformed *S. typhimurium* were grown in modified Luria–Bertani medium containing ampicillin (100  $\mu\text{g}/\text{mL}$ ) until the late log phase and then diluted in DMEM before administration to the mammalian cell cultures. To calculate colony-forming units (CFU)/mL, the following conversion was used:  $\text{OD}_{600}$  of 1 =  $10^9$  CFU/mL. After coculturing the tumor cells and bacteria, the extracellular bacteria were removed using kanamycin (100  $\mu\text{g}/\text{mL}$ ). To confirm infection efficiency, the percentage of tdTomato<sup>+</sup> B16F10 cells was evaluated using a FACSCanto II flow cytometer (BD Biosciences, San Diego, CA, USA).

## Evaluation of caspase-1 activity

To measure caspase-1 activation, an anticaspase-1 fluorochrome-labeled inhibitor of caspases (FLICA) probe (FAM-YVAD-FMK; Immunochemistry Technologies, Bloomington, MN, USA) was added in uninfected and infected B16F10 cell cultures, according to the manufacturer's instructions.

## Evaluation of micropinocytosis

B16F10 cells were inoculated with VNP-tdT in the presence of Lucifer Yellow (1.5 mg/mL; Invitrogen, Waltham, MA, USA). Lucifer Yellow was then removed, and the cells were washed three times with DMEM containing kanamycin (100  $\mu\text{g}/\text{mL}$ ). Phase-contrast and fluorescent images of the live cells were taken using an Olympus CKX53 microscope equipped with a digital camera.

## Gene expression profiling

Total RNA was isolated from uninfected and infected B16F10 cells using the RNeasy Plus Mini Kit (Qiagen, Venlo, The Netherlands) according to the manufacturer's protocol. cDNA was synthesized using the GeneChip Whole Transcript (WT) Amplification Kit (Applied Biosystems, Waltham, MA, USA) as instructed by the manufacturer. The sense cDNA was then fragmented and biotin-labeled with terminal deoxynucleotidyl transferase using the GeneChip WT Terminal Labeling Kit. Approximately, 5.5  $\mu\text{g}$  of the labeled DNA target was then hybridized to the Affymetrix GeneChip Array at 45 °C for 16 h. Hybridized arrays were washed and stained on a GeneChip Fluidics Station 450 and scanned on a GCS3000 Scanner (Affymetrix, Santa Clara, CA, USA). The expression profiles among samples were analyzed using mouse Clariom S Assays (Applied Biosystems).

## Detection of extracellular ATP leakage

Extracellular ATP in culture supernatants was measured at the indicated time points using the Celltiter-Glo 2.0 ATP Assay Kit (Promega, Madison, WI, USA) according to the manufacturer's instructions. Luminescence was measured using the VarioScan Flash plate reader (Thermo Scientific, Waltham, MA, USA).

## Flow cytometry

For the detection of CD47 expression, uninfected and infected B16F10 cells were stained with an Alexa647-conjugated

antimouse CD47 antibody (Ab; clone miap301; BioLegend, San Diego, CA, USA) and the LIVE/DEAD Fixable Near-IR Dead Cell Stain Kit (Invitrogen).

For the detection of CD86 expression and cell surface calreticulin exposure, Raw264.7 mouse macrophages were cocultured with VNP-tdT-infected or uninfected B16F10 cells for 18 h at a ratio of 1:1. At the endpoint of the incubation, the cells were harvested and stained with the LIVE/DEAD Fixable Near-IR Dead Cell Stain Kit (Invitrogen), a fluorescein isothiocyanate (FITC)-conjugated antimouse CD45 monoclonal Ab (mAb; clone 30-F11; BioLegend), a PE-Cy7-conjugated antimouse CD86 mAb (clone GL-1; BioLegend), or an anticalreticulin polyclonal Ab (pAb; ab2907; Abcam, Cambridge, UK) with an Alexa647-conjugated secondary antirabbit IgG Ab (BioLegend). To detect intracellular *Salmonella*, infected or uninfected B16F10 cells were fixed and permeabilized with the FOXP3 Fix/Perm Buffer Set (BioLegend) and stained with anti-*S. typhimurium* mAb (clone 1E6; Santa Cruz Biotechnology, Dallas, TX, USA) with an Alexa488-conjugated secondary antimouse IgG Ab (BioLegend). Flow cytometry data were acquired on a FACSCanto II flow cytometer and analyzed using FlowJo software (BD Biosciences).

## In vitro phagocytosis assay

In vitro phagocytosis assays were performed, as previously described (48, 65). Briefly, VNP-tdT-infected or uninfected B16F10-ZsGreen cells ( $1 \times 10^5$ /well) were cocultured with Raw264.7 mouse macrophages or BMDCs at a ratio of 1:1 for 18 h. At the endpoint of the incubation, the cells were harvested and stained with a Alexa647-conjugated antimouse CD45 mAb (for Raw264.7 cells; clone 30-F11; BioLegend) or a Alexa647-conjugated antimouse CD11c mAb (for BMDCs; clone N418; BioLegend). Phagocytosis was assessed using a flow cytometer. Colocalization of the fluorescence of Alexa647 and ZsGreen indicated the phagocytosis of tumor cells.

## Tumor model

Mice were subcutaneously injected in the flank with: (i)  $2 \times 10^5$  uninfected; (ii)  $2 \times 10^5$  uninfected and  $5 \times 10^4$  infected; (iii)  $2 \times 10^5$  uninfected and  $2 \times 10^5$  infected; or (iv)  $2 \times 10^5$  infected tumor cells. Tumor size (length  $\times$  width) was measured every 2–3 days with a caliper. Mice were sacrificed when the tumor area reached 150 mm<sup>2</sup> or upon ulceration.

## In vitro cytotoxicity assay

Mice were subcutaneously immunized with  $2 \times 10^5$  VNP-tdT-infected B16F10 cells on days 0 and 7. On day 14, cells from the draining lymph node (dLn) were prepared as effector cells. These effector cells were activated in vitro for 6 days in the presence of IL-2 (175 IU/mL in KBM550 medium; KOHJIN BIO, Saitama, Japan) and were used as activated effector cells.

In vitro cytotoxicity assays were performed, as previously described (66). Briefly, B16F10-ZsGreen cells ( $1 \times 10^5$ /well) were cocultured with activated effector cells (effector-to-target ratio = 40:1) in wells of a round-bottom, 96-well, low-detach plate, in the presence of propidium-iodide (PI) at 37 °C for 4 h. After incubation, the ZsGreen-positive target cells were analyzed for PI staining using a FACSCanto II flow cytometer (BD Biosciences). Percentage cell death (% CD) was calculated as  $(\text{PI}^+ \text{ZsGreen}^+ \text{ target cells} / \text{total ZsGreen}^+ \text{ target cells}) \times 100$ . Percentage-specific cell death (%SCD) was calculated according to the formula: % SCD =  $(\text{sample \% CD} - \text{spontaneous \% CD}) / (100 - \text{spontaneous \% CD})$ .

CD) × 100. Spontaneous % CD represents the % CD in the culture of target cells alone.

## Detection of melanoma-antigen-specific T-cell proliferation in vivo

Pmel-1 mice were subcutaneously immunized with  $2 \times 10^5$  VNP-tdT-infected B16F10 cells on days 0 and 7. On day 14, the dLn cells were isolated after staining with a gp100-MHC-tetramer, a PerCP-conjugated antimouse CD44 mAb (clone IM7; BioLegend), and a PE-C7-conjugated antimouse CD8 mAb (clone 53-6.7; BioLegend). A PE-conjugated H-2D<sup>b</sup>-HCV630 MHC-tetramer (67) was used as a staining control to detect non-specific MHC-tetramer binding. After cell surface staining, cells were fixed and permeabilized with the FOXP3 Fix/Perm Buffer Set (BioLegend) and stained with an APC-conjugated anti-Ki67 mAb (clone 16A8; BioLegend). Flow cytometry data were acquired on a FACSCanto II flow cytometer and analyzed using FlowJo software (BD Biosciences); the gating strategy is shown in Fig. S9.

## Statistical analysis

All statistical analyses were performed using GraphPad Prism 9 (GraphPad Software, Boston, MA, USA), and the threshold used to define statistical significance was a *P*-value <0.05.

## Acknowledgments

The authors thank Ms Kanae Hino for administrative and technical assistance. The authors are extremely grateful to the Saitama Medical University Biomedical Research Center for its excellent service. Finally, they thank Edanz (<https://jp.edanz.com/ac>) for editing a draft of this manuscript.

## Supplementary Material

Supplementary material is available at PNAS Nexus online.

## Funding

This work was supported in part by JSPS KAKENHI Grant-in-Aid for Scientific Research (C) (grant number 21K08333 to Y.H. and 22K08437 to T.M.).

## Author Contributions

Y.H. conceived the study, designed, and performed the experiments, analyzed the data, and produced the figures. Y.H. and T.M. wrote the manuscript. A.N. performed image acquisition. T.I. and T.M. helped with the experimental design. T.M. provided modified cell resources and supervised the project. All authors read and approved the final version of the manuscript.

## Data Availability

Microarray data are available on Figshare with doi:[10.6084/m9.figshare.22723234](https://doi.org/10.6084/m9.figshare.22723234).

## References

- 1 Bruni D, Angell HK, Galon J. 2020. The immune contexture and Immunoscore in cancer prognosis and therapeutic efficacy. *Nat Rev Cancer*. 20:662–680.
- 2 Fridman WH, Zitvogel L, Sautès-Fridman C, Kroemer G. 2017. The immune contexture in cancer prognosis and treatment. *Nat Rev Clin Oncol*. 14:717–734.
- 3 Apetoh L, Tesniere A, Ghiringhelli F, Kroemer G, Zitvogel L. 2008. Molecular interactions between dying tumor cells and the innate immune system determine the efficacy of conventional anti-cancer therapies. *Cancer Res*. 68:4026–4030.
- 4 Apetoh L, et al. 2007. Toll-like receptor 4-dependent contribution of the immune system to anticancer chemotherapy and radiotherapy. *Nat Med*. 13:1050–1059.
- 5 Korbek M, Kros J, Kros J, Dougherty GJ. 1996. The role of host lymphoid populations in the response of mouse EMT6 tumor to photodynamic therapy. *Cancer Res*. 56:5647–5652.
- 6 Chen DS, Mellman I. 2013. Oncology meets immunology: the cancer-immunity cycle. *Immunity*. 39:1–10.
- 7 Fucikova J, et al. 2020. Detection of immunogenic cell death and its relevance for cancer therapy. *Cell Death Dis*. 11:1013.
- 8 Liu CC, et al. 2016.  $\alpha$ -Integrin expression and function modulates presentation of cell surface calreticulin. *Cell Death Dis*. 7:e2268.
- 9 Obeid M, et al. 2007. Calreticulin exposure dictates the immunogenicity of cancer cell death. *Nat Med*. 13:54–61.
- 10 Fang H, et al. 2014. TLR4 is essential for dendritic cell activation and anti-tumor T-cell response enhancement by DAMPs released from chemically stressed cancer cells. *Cell Mol Immunol*. 11:150–159.
- 11 Tesniere A, et al. 2010. Immunogenic death of colon cancer cells treated with oxaliplatin. *Oncogene*. 29:482–491.
- 12 Bonaventura P, et al. 2019. Cold tumors: a therapeutic challenge for immunotherapy. *Front Immunol*. 10:168.
- 13 Martins I, et al. 2014. Molecular mechanisms of ATP secretion during immunogenic cell death. *Cell Death Differ*. 21:79–91.
- 14 Ghiringhelli F, et al. 2009. Activation of the NLRP3 inflammasome in dendritic cells induces IL-1 $\beta$ -dependent adaptive immunity against tumors. *Nat Med*. 15:1170–1178.
- 15 Jie X, et al. 2022. Targeting KDM4C enhances CD8<sup>+</sup> T cell mediated antitumor immunity by activating chemokine CXCL10 transcription in lung cancer. *J Immunother Cancer*. 10:e003716.
- 16 Galluzzi L, Buqué A, Kepp O, Zitvogel L, Kroemer G. 2017. Immunogenic cell death in cancer and infectious disease. *Nat Rev Immunol*. 17:97–111.
- 17 Zhang H, Zoued A, Liu X, Sit B, Waldor MK. 2020. Type I interferon remodels lysosome function and modifies intestinal epithelial defense. *Proc Natl Acad Sci U S A*. 117:29862–29871.
- 18 Gasper NA, Petty CC, Schrum LW, Marriott I, Bost KL. 2002. Bacterium-induced CXCL10 secretion by osteoblasts can be mediated in part through toll-like receptor 4. *Infect Immun*. 70:4075–4082.
- 19 Wang D, Wei X, Kalvakolanu DV, Guo B, Zhang L. 2021. Perspectives on oncolytic *Salmonella* in cancer immunotherapy—a promising strategy. *Front Immunol*. 12:615930.
- 20 McCarthy EF. 2006. The toxins of William B. Coley and the treatment of bone and soft-tissue sarcomas. *Iowa Orthop J*. 26:154–158.
- 21 Zhou S, Gravekamp C, Bermudes D, Liu K. 2018. Tumour-targeting bacteria engineered to fight cancer. *Nat Rev Cancer*. 18:727–743.
- 22 Phan T, et al. 2020. *Salmonella*-mediated therapy targeting indoleamine 2, 3-dioxygenase 1 (IDO) activates innate immunity and mitigates colorectal cancer growth. *Cancer Gene Ther*. 27:235–245.
- 23 Chowdhury S, et al. 2019. Programmable bacteria induce durable tumor regression and systemic antitumor immunity. *Nat Med*. 25:1057–1063.
- 24 Gurbatri CR, Arpaia N, Danino T. 2022. Engineering bacteria as interactive cancer therapies. *Science*. 378:858–864.

- 25 Badie F, et al. 2021. Use of *Salmonella* bacteria in cancer therapy: direct, drug delivery and combination approaches. *Front Oncol.* 11:624759.
- 26 Liang K, et al. 2019. Genetically engineered *Salmonella typhimurium*: recent advances in cancer therapy. *Cancer Lett.* 469:102–110.
- 27 Hernández-Luna MA, Luria-Pérez R. 2018. Cancer immunotherapy: priming the host immune response with live attenuated *Salmonella enterica*. *J Immunol Res.* 2018:2984247.
- 28 Zhang Y, et al. 2012. Determination of the optimal route of administration of *Salmonella typhimurium* A1-R to target breast cancer in nude mice. *Anticancer Res.* 32:2501–2508.
- 29 Casey DL, et al. 2021. TP53 mutations increase radioresistance in rhabdomyosarcoma and Ewing sarcoma. *Br J Cancer.* 125:576–581.
- 30 Eggermont AM, Spatz A, Robert C. 2014. Cutaneous melanoma. *Lancet.* 383:816–827.
- 31 Schiff D, Sheehan JP. 2012. SBRT and spinal metastasis: finding its niche. *Lancet Oncol.* 13:328–329.
- 32 Franchi L, Kanneganti TD, Dubyak GR, Núñez G. 2007. Differential requirement of P2X7 receptor and intracellular K<sup>+</sup> for caspase-1 activation induced by intracellular and extracellular bacteria. *J Biol Chem.* 282:18810–18818.
- 33 Lara-Tejero M, et al. 2006. Role of the caspase-1 inflammasome in *Salmonella typhimurium* pathogenesis. *J Exp Med.* 203:1407–1412.
- 34 Maltese WA, Overmeyer JH. 2014. Methuosis: nonapoptotic cell death associated with vacuolization of macropinosome and endosome compartments. *Am J Pathol.* 184:1630–1642.
- 35 Overmeyer JH, Kaul A, Johnson EE, Maltese WA. 2008. Active ras triggers death in glioblastoma cells through hyperstimulation of micropinocytosis. *Mol Cancer Res.* 6:965–977.
- 36 Fujii M, Kawai K, Egami Y, Araki N. 2013. Dissecting the roles of Rac1 activation and deactivation in micropinocytosis using microscopic photo-manipulation. *Sci Rep.* 3:2385.
- 37 Bhanot H, Young AM, Overmeyer JH, Maltese WA. 2010. Induction of nonapoptotic cell death by activated Ras requires inverse regulation of Rac1 and Arf6. *Mol Cancer Res.* 8:1358–1374.
- 38 Sun ZJ, et al. 2008. Involvement of Cyr61 in growth, migration, and metastasis of prostate cancer cells. *Br J Cancer.* 99:1656–1667.
- 39 Emre Y, Imhof BA. 2014. Matricellular protein CCN1/CYR61: a new player in inflammation and leukocyte trafficking. *Semin Immunopathol.* 36:253–259.
- 40 Haseley A, et al. 2012. Extracellular matrix protein CCN1 limits oncolytic efficacy in glioma. *Cancer Res.* 72:1353–1362.
- 41 Thorne AH, et al. 2014. Role of cysteine-rich 61 protein (CCN1) in macrophage-mediated oncolytic herpes simplex virus clearance. *Mol Ther.* 22:1678–1687.
- 42 Marin I, et al. 2023. Cellular senescence is immunogenic and promotes anti-tumor immunity. *Cancer Discov.* 13:410–431.
- 43 Sriram G, et al. 2021. The injury response to DNA damage in live tumor cells promotes antitumor immunity. *Sci Signal.* 14:eabc4764.
- 44 Elliott MR, et al. 2009. Nucleotides released by apoptotic cells act as a find-me signal to promote phagocytic clearance. *Nature.* 461:282–286.
- 45 Krysko DV, et al. 2012. Immunogenic cell death and DAMPs in cancer therapy. *Nat Rev Cancer.* 12:860–875.
- 46 Feng M, et al. 2019. Phagocytosis checkpoints as new targets for cancer immunotherapy. *Nat Rev Cancer.* 19:568–586.
- 47 Gardai SJ, et al. 2005. Cell-surface calreticulin initiates clearance of viable or apoptotic cells through trans-activation of LRP on the phagocyte. *Cell.* 123:321–334.
- 48 Feng M, et al. 2015. Macrophages eat cancer cells using their own calreticulin as a guide: roles of TLR and Btk. *Proc Natl Acad Sci U S A.* 112:2145–2150.
- 49 Feng M, et al. 2018. Programmed cell removal by calreticulin in tissue homeostasis and cancer. *Nat Commun.* 9:3194.
- 50 Phan TX, et al. 2015. Activation of inflammasome by attenuated *Salmonella typhimurium* in bacteria-mediated cancer therapy. *Microbiol Immunol.* 59:664–675.
- 51 Ji Y, et al. 2014. Identification of the genomic insertion site of Pmel-1 TCR  $\alpha$  and  $\beta$  transgenes by next-generation sequencing. *PLoS One.* 9:e96650.
- 52 Overwijk WW, et al. 2003. Tumor regression and autoimmunity after reversal of a functionally tolerant state of self-reactive CD8<sup>+</sup> T cells. *J Exp Med.* 198:569–580.
- 53 Howard E, et al. 2021. IL-10 production by ILC2s requires Blimp-1 and cMaf, modulates cellular metabolism, and ameliorates airway hyperreactivity. *J Allergy Clin Immunol.* 147:1281–1295.e5.
- 54 Huang L, et al. 2021. Expression of tdTomato and luciferase in a murine lung cancer alters the growth and immune microenvironment of the tumor. *PLoS One.* 16(8):e0254125.
- 55 Yuzhakova DV, et al. 2015. CT26 murine colon carcinoma expressing the red fluorescent protein KillerRed as a highly immunogenic tumor model. *J Biomed Opt.* 20(8):88002.
- 56 Bloy N, et al. 2017. Immunogenic stress and death of cancer cells: contribution of antigenicity vs adjuvanticity to immunosurveillance. *Immunol Rev.* 280:165–174.
- 57 Belderbos RA, Aerts JGJV, Vroman H. 2019. Enhancing dendritic cell therapy in solid tumors with immunomodulating conventional treatment. *Mol Ther Oncolytics.* 13:67–81.
- 58 Geyer RJ, Tobet R, Berlin RD, Srivastava PK. 2013. Immune response to mutant neo-antigens: cancer's lessons for aging. *Oncoimmunology.* 2:e26382.
- 59 Ochsenbein AF, et al. 1999. Immune surveillance against a solid tumor fails because of immunological ignorance. *Proc Natl Acad Sci U S A.* 96:2233–2238.
- 60 Mills KH. 2011. TLR-dependent T cell activation in autoimmunity. *Nat Rev Immunol.* 11:807–822.
- 61 Kamradt T, Göggel R, Erb KJ. 2005. Induction, exacerbation and inhibition of allergic and autoimmune diseases by infection. *Trends Immunol.* 26:260–267.
- 62 Overwijk WW, et al. 1998. Gp100/pmel 17 is a murine tumor rejection antigen: induction of “self”-reactive, tumoricidal T cells using high-affinity, altered peptide ligand. *J Exp Med.* 188:277–286.
- 63 Paulos CM, et al. 2007. Microbial translocation augments the function of adoptively transferred self/tumor-specific CD8<sup>+</sup> T cells via TLR4 signaling. *J Clin Invest.* 117:2197–2204.
- 64 Galluzzi L, et al. 2020. Consensus guidelines for the definition, detection and interpretation of immunogenic cell death. *J Immunother Cancer.* 8:e000337.
- 65 Inoue S, et al. 2020. Immune checkpoint inhibition followed by tumor infiltration of dendritic cells in murine neuro-2a neuroblastoma. *J Surg Res.* 253:201–213.
- 66 Takagi A, Horiuchi Y, Matsui M. 2017. Characterization of the flow cytometric assay for ex vivo monitoring of cytotoxicity mediated by antigen-specific cytotoxic T lymphocytes. *Biochem Biophys Res Commun.* 492:27–32.
- 67 Horiuchi Y, et al. 2014. Effect of the infectious dose and the presence of hepatitis C virus core gene on mouse intrahepatic CD8 T cells. *Hepatol Res.* 44:E240–E252.